HHS Public Access

Author manuscript

Breast Cancer Res Treat. Author manuscript; available in PMC 2016 December 28.

Published in final edited form as:

Breast Cancer Res Treat. 2015 May ; 151(1): 57–73. doi:10.1007/s10549-015-3365-8.

Metabotropic glutamate receptor 1 disrupts mammary acinar architecture and initiates malignant transformation of mammary epithelial cells

Jessica L. F. Teh[1], **Raj Shah**[1], **Stephanie La Cava**[1], **Sonia C. Dolfi**[2], **Madhura S. Mehta**[2], **Sameera Kongara**[2], **Sandy Price**[2], **Shridar Ganesan**[2], **Kenneth R. Reuhl**[3], **Kim M. Hirshfield**[2], **Vassiliki Karantza**[2,4], and **Suzie Chen**[1,2]

[1]Susan Lehman Cullman Laboratory for Cancer Research, Ernest Mario School of Pharmacy, Rutgers, The State University of New Jersey, Piscataway, NJ 08854, USA

[2]Rutgers Cancer Institute of New Jersey, Rutgers, The State University of New Jersey, New Brunswick, NJ 08903, USA

[3]Department of Pharmacology and Toxicology, Ernest Mario School of Pharmacy, Rutgers, The State University of New Jersey, Piscataway, NJ 08854, USA

[4]Department of Medicine-Medical Oncology, Rutgers Cancer Institute of New Jersey, Rutgers, The State University of New Jersey, 195 Little Albany Street, New Brunswick, NJ 08901, USA

Abstract

Metabotropic glutamate receptor 1 (mGluR1/Grm1) is a member of the G-protein-coupled receptor superfamily, which was once thought to only participate in synaptic transmission and neuronal excitability, but has more recently been implicated in non-neuronal tissue functions. We previously described the oncogenic properties of Grm1 in cultured melanocytes in vitro and in spontaneous melanoma development with 100 % penetrance in vivo. Aberrant mGluR1 expression was detected in 60–80 % of human melanoma cell lines and biopsy samples. As most human cancers are of epithelial origin, we utilized immortalized mouse mammary epithelial cells (iMMECs) as a model system to study the transformative properties of Grm1. We introduced Grm1 into iMMECs and isolated several stable mGluR1-expressing clones. Phenotypic alterations in mammary acinar architecture were assessed using three-dimensional morphogenesis assays. We found that mGluR1-expressing iMMECs exhibited delayed lumen formation in association with decreased central acinar cell death, disrupted cell polarity, and a dramatic increase in the activation of the mitogen-activated protein kinase pathway. Orthotopic implantation of mGluR1-expressing iMMEC clones into mammary fat pads of immunodeficient nude mice resulted in mammary tumor formation in vivo. Persistent mGluR1 expression was required for the maintenance of the tumorigenic phenotypes in vitro and in vivo, as demonstrated by an inducible Grm1-silencing RNA system. Furthermore, mGluR1 was found be expressed in human breast cancer cell lines and

Correspondence to: Vassiliki Karantza; Suzie Chen.

Conflict of interest The authors declare no conflict of interest.

Electronic supplementary material The online version of this article (doi:10.1007/s10549-015-3365-8) contains supplementary material, which is available to authorized users.

breast tumor biopsies. Elevated levels of extracellular glutamate were observed in mGluR1-expressing breast cancer cell lines and concurrent treatment of MCF7 xenografts with glutamate release inhibitor, riluzole, and an AKT inhibitor led to suppression of tumor progression. Our results are likely relevant to human breast cancer, highlighting a putative role of mGluR1 in the pathophysiology of breast cancer and the potential of mGluR1 as a novel therapeutic target.

Keywords

Metabotropic glutamate receptor 1; Mammary epithelial cells; Breast cancer; Oncogene; Cell transformation

Introduction

Our understanding of glutamatergic signaling in tumorigenesis has steadily gained a foothold over the last decade. Interest in the aberrant signaling exerted by glutamate receptors in non-neuronal cells was reawakened by the recent discovery of oncogenic mutations in human melanoma, such as GRIN2A and GRM3, which encode the NMDA receptor subunit ε-1 and the metabotropic glutamate receptor 3, respectively [1, 2]. Our laboratory was the first to establish the role of metabotropic glutamate receptor 1, (gene: Grm1, mouse and GRM1, human; protein:mGluR1) in melanomagenesis in vivo by demonstrating that ectopic expression of mGluR1 alone is sufficient to induce melanocytic neoplasia [3]. Additionally, stable mGluR1-expressing mouse melanocytic clones are fully transformed and aggressively tumorigenic in vivo [4]. Furthermore, our observations suggest that constitutive stimulation of mGluR1 by its natural ligand, glutamate, is required to maintain transformed phenotypes in vitro/in vivo through the establishment of autocrine/paracrine loops.

Recent studies have implicated mGluR1 in epithelial tumorigenesis, as mGluR1 was reported to regulate proliferation in triple-negative breast cancer cells and the tumor inhibitory effects of mGluR1 antagonists were shown in an MDA-MB-231 xenograft tumor model [5]. Furthermore, two polymorphic variants of GRM1, rs6923492, and rs362962, were found associated with breast cancer phenotypes [6]. In addition, low mGluR1 expression correlated with a longer distant metastasis-free survival (DMFS) in patients with estrogen receptor (ER)-positive breast cancers treated with tamoxifen, suggesting a functional role for mGluR1 in the setting of active hormone signaling [6]. In prostate cancer patients, serum glutamate levels correlated with Gleason score and high levels of mGluR1 expression were detected in primary and metastatic tissues [7]. Our group previously reported that exogenous Grm1 transforms immortalized baby mouse kidney (iBMK) cells in vitro and in vivo, and reported functional glutamate signaling in the corresponding human tumor type, renal cell carcinoma [8]. However, neither the mechanism, by which Grm1 mediates mammary epithelial cell transformation, nor whether sustained mGluR1 expression is required for breast tumorigenesis are well understood.

Breast cancer is the most common malignancy afflicting women in the United States, ranking second in the number of cancer deaths among women and preceded only by lung cancer [9]. The normal breast comprises a network of ducts and lobules, which ultimately

give rise to terminal ductal lobular unit (TDLU) structures. It is within the epithelium of these units that the most invasive form of breast cancer is thought to arise. The TDLU is made up of a collection of acinar structures consisting of a single layer of polarized luminal epithelial cells surrounding a hollow lumen. Three-dimensional (3D) epithelial culture systems, which allow epithelial cells to organize into structures that resemble in vivo ductal architecture, are useful for elucidating the functions of cancer genes and pathways in a biologically relevant context. One such model involves the use of immortalized mouse mammary epithelial cells (iMMECs) [10], which form polarized hollow acini in the presence of extracellular matrix, similar to the well-characterized non-malignant human breast epithelial cell line MCF10A [11], and have been successfully used to study breast cancer-promoting functions [12, 13]. To directly investigate the role of mGluR1 in mammary tumorigenesis, we isolated several independent stable iMMEC clones with exogenous Grm1. We now report that by disrupting acinar morphogenesis, Grm1 induces transformation of mammary epithelial cells in vitro and promotes mammary tumorigenesis in vivo. Furthermore, modulation of mGluR1 signaling suppresses tumor growth of ER-positive human breast cancer cell xenografts in nude mice, suggesting that this pathway plays an important role in breast cancer pathogenesis and could be pharmacologically targeted for breast cancer treatment.

Materials and methods

Antibodies, reagents, and western immunoblots

Antibodies to phosphorylated-AKT (Ser473), AKT, phosphorylated ERK1/2 (Thr202/Tyr204), and ERK1/2 were purchased from Cell Signaling (Danvers, MA). Anti-mGluR1 antibody (mouse) was purchased from BD Biosciences (Franklin Lakes, NJ), anti-mGluR1 antibody (human) was purchased from Novus Biologicals (Littleton, CO) and SDIX (Newark, DE). Monoclonal anti-α-tubulin antibody and doxycycline hyclate were purchased from Sigma (St. Louis, MO). Secondary antibodies, donkey anti-Rabbit IgG Antibody, -HRP conjugate and Goat Anti-Mouse IgG, -H&L Chain Specific Peroxidase Conjugate, and Luminata Western HRP substrates were purchased from Millipore (Billerica, MA). Riluzole was purchased from Sigma (St. Louis, MO), BAY 36-7620 was purchased from Tocris (Bristol, UK), and MK-2206 was generously provided by Merck & Co., Inc. and the National Cancer Institute, National Institutes of Health.

Protein lysates were prepared as described previously [14]. Briefly, media were removed and cells were washed once with ice-cold phosphate buffered saline (PBS). After removal of PBS, extraction buffer was added directly to the plates and cells were collected with a cell scraper. Cell extracts were incubated on ice for 20 min. Cell debris was removed by centrifugation at 14,000×*g* at 4 °C for 20 min, supernatant was collected to measure protein concentration with Detergent Compatible Protein Assay (Bio-Rad Laboratories, Hercules, CA), and 25 μg of protein was routinely used for Western immunoblot analysis.

Cell culture, transfection, and generation of stable cell lines

iMMECs were generated from mouse mammary epithelial cells isolated from young, C57BL/6 virgin female mice, and immortalized through the inactivation of Rb and p53

pathways as previously described [10, 15]. Cells were maintained in regular iMMEC growth medium (F12 medium supplemented with 5 μg/ml insulin, 1 μg/ml hydrocortisone, and 5 μg/ml EGF) with 10 % FBS. Breast cancer cells were maintained in RPMI supplemented with 10 % FBS except BT474 which was maintained in DMEM supplemented with 10 % FBS.

Coding sequence for the full-length α form of Grm1 was subcloned from mouse brain cDNA library [16] into mammalian expression vector pCI-neo (Promega, Madison, WI). A total of 2.5 μg Grm1 cDNA was transfected into iMMECs (3×10^5 cells) using DOTAP transfection reagent (Roche, Mannheim, Germany). Stable Grm1-transfectants were selected using 100 μg/ml neomycin in regular iMMEC growth medium. MCF12A cells were transfected with pCI-neo plasmid with and without cDNA encoding human GRM1α (NCBI accession NM_001278064.1). Receptor expression was confirmed by Western blotting.

TetR plasmid (neomycin-resistant) was co-transfected with Zeocin plasmid and TetR clones were selected with Zeocin (Invitrogen, Grand Island, NY) at a concentration of (300 μg/ml). siGrm1 or siGFP sequence was cloned into the inducible siRNA expression vector pRNATin-H1.1/Hygro (GenScript, Piscataway, NJ). Stable siRNA/TetR-transfected iMMEC-Grm1 clones were selected in Hygromycin B (Invitrogen, Grand Island, NY) at a concentration of (50 μg/ml). siGRM1-MCF7 clones were selected in neomycin (300 μg/ml) and Hygromycin B (50 μg/ml). For induction of siGrm1, 4 μg/ml of doxycycline was added a day after plating and medium was replaced every 4 days in 2D or 3D cultures.

The 3D cultures of iMMECs were generated as previously described [10]. Mammary acini were grown in iMMEC growth medium and 2 % growth factor-reduced matrigel (BD Biosciences, Franklin Lakes, NJ). The medium was replaced every 4 days.

3D morphogenesis assay and scoring of 3D structures

Mammary acini were fixed and processed for immunofluorescence as previously described [10]. Acini were incubated with primary antibodies overnight at 4 °C, washed, and then incubated with fluorescein- or rhodamine-coupled secondary antibodies for 2 h at room temperature. Finally, acini were stained with TO-PRO-3, washed, and mounted with Prolong anti-fade. Confocal laser scanning was carried out with a Nikon D-Eclipse C1 Confocal Microscope. 3D structures were scored for lumen formation based on the resemblance to the 3D structure integrity of vector images (Day 21 time point) shown in Fig. 1c. Over 300 structures were scored for lumen formation.

Antibody	Function	Normal localization	Source	Species
Cleaved Caspase-3	Apoptosis maker	Apoptotic cells in luminal space	Cell signaling	Rabbit
B-Catenin	Cell–cell junction	Basolateral	Zymed lab	Mouse
TO-PRO-3	Nuclear counterstain	Nuclei	Invitrogen	NA
GM130	Apical polarity	Golgi (apically located)	BD	Mouse
Ki-67	Proliferation marker	Nuclei of proliferating cells	DakoCytomation	Rat
Phospho-ERK	ERK activation	Cytosol and nucleus	Cell signaling	Rabbit
Total ERK	ERK activation control	Cytosol and nucleus	Cell signaling	Rabbit

Tumorigenicity assays

iMMECs-expressing mGluR1 or empty vector was harvested by trypsinization and resuspended in PBS (10^7 cells/ml). Orthotopic mammary gland implantation of iMMECs was performed according to our Institutional Animal Care and Use Committee approved protocol. 5–6-week-old immunodeficient nude female mice were anesthetized with Avertin. A small incision was made to expose the second pair of mammary fat pads on both sides and each mammary gland pad was subjected to implantation with 10^6 cells. The incision was closed with surgical clips that were removed 10 days later. Tumor growth was monitored weekly with a vernier caliper and calculated with the formula ($d^2 \times D/2$) as described [17]. Studies were terminated as soon as tumor volumes reached maximum permitted size. Similar protocol was carried out for the following in vivo studies: siGrm1/TetR iMMECs (10^8 cells/ml), siGRM1/TetR MCF7 (5×10^7 cells/ml), and MCF7 (5×10^7 cells/ml). For the siGrm1/TetR studies, once tumor volumes reached 10 mm^3, mice were divided into two treatment groups. Doxycycline (0.2 % w/v) was included in the drinking water of doxycycline treatment groups to induce siGrm1 expression and the drinking water was replaced twice a week. For siGRM1/TetR MCF7 and MCF7 xenografts, 2.5 mg 90-day release 17β-estradiol pellet (Innovative Research of America, Sarasota, Florida) was implanted into the interscapular region of each mouse.

For the MCF7 xenograft study, once MCF7 tumor volumes reached 10 mm^3, mice were divided into four treatment groups and received vehicle (DMSO), riluzole (10 mg/kg), MK-2206 (30 mg/kg), or the combination of riluzole (5 mg/kg) and MK-2206 (15 mg/kg) by oral gavage, daily for riluzole and twice a week for MK2206. The experiments were terminated when the xenografts on the no treatment or vehicle group reached the maximum permitted size.

Immunohistochemistry

The human tissues were obtained from the Biospecimen Retrieval Service at Rutgers Cancer Institute of NJ (RCINJ). RCINJ Histopathology and Imaging Core performed the IHC for mGluR1 and unbiased quantitative assessment of IHC staining was completed using a digital Aperio ScanScopeGL system and ImageScope software (v10.1.3.2028) (Aperio Technologies Inc., Vista, CA) as described [18]. Images were taken using Olympus BX51 microscope and camera system.

Cell proliferation/viability (MTT) assay

Each cell line was cultured in 96-well plates at 2×10^3 cells per well with the following conditions: no treatment or doxycycline (4 μg/ml). Viable cells were measured at Day 4 and Day 7. At designated time points, 0.1 volumes of 5 mg/ml Thiazolyl Blue Tetrazolium Bromide (Sigma, St. Louis, MO) in 1X PBS were added to growth medium, incubated for 4 h at 37 °C, and then solubilized overnight with equal volume of 10 % sodium dodecyl sulfate/0.1 N HCl. A 96-well plate reader (Infinite 200 Tecan USA, Durham, NC, USA) was used to measure absorbance at 550 nM with a reference wavelength of 750 nM.

Glutamate release assay

Cells were seeded at 4×10^3 per well and cultured in 200 μl glutamate/glutamine-free medium with 10 % dialyzed FBS. At measurement, half of the volume was removed from each well for glutamate assay and cell viability immediately assessed by MTT assay. Amplex Red Glutamic Acid/Glutamate Oxidase Assay Kit (Invitrogen, Carlsbad, CA, USA) and Glutamate Assay Kit (Sigma, St. Louis, MO) was used to measure glutamate concentration in culture medium.

Cell cycle analysis

Cells were plated at 1×10^6 per 100 mm dish and treated with 50 μM riluzole or vehicle (dimethyl sulfoxide) for 24–48 h. Adherent and floating cells were pooled, pelleted, washed twice with ice-cold 1X PBS, and fixed by dropwise addition of ice-cold 70 % ethanol while mixing and stored at 20 °C. Fixed cells were washed twice with and resuspended in 1X PBS, treated with RNase A solution (Sigma, St. Louis, MO) at 100 mg/ml and stained with propidium iodide (Sigma, St Louis, MO) at 10 mg/ml for 30 min. Cell cycle analysis was performed on a Coulter Cytomics FC500 Flow Cytometer (Beckman Coulter, Fullerton, CA, USA) at the Analytical Cytometry Core Facility, Rutgers University.

Analysis of in vivo synergy data

The nature of the interaction between riluzole and MK-2206 was analyzed by the combination index method [19]. The combination index was calculated using equation:

$$\text{Combination Index} = \left[\text{IC}_{\text{Ril,Comb}}/\text{IC}_{\text{Ril}}\right] + \left[\text{IC}_{\text{MK,Comb}}/\text{IC}_{\text{MK}}\right]$$

Here IC_{Ril} and IC_{MK} are the concentrations of riluzole and MK-2206 needed to produce a given level of cytotoxicity when used alone, and $IC_{Ril,\ Comb}$ and $IC_{MK,\ Comb}$ are the concentrations needed to produce the same effect when used in combination. A combination index value of 1 indicates additive interaction, values less than 1 indicate synergistic interaction, and values greater than 1 indicate antagonistic interaction.

Affymetrix GeneChip

Seventeen ER-positive and thirty-five ER-negative breast cancer cell lines were evaluated for GRM1 expression using publicly available data from Neve et al. [20]. Gene expression was measured using three distinct Affymetrix probe sets (“207299_s_at,” “210939_s_at,” and “210940_s_at”). Using the expression value from three probes within each cell line, an average expression was calculated. For ease of visualization, data are represented as a function of ER status.

Statistical analyses

Statistical analysis was done using a two-tailed test assuming unequal variance with error bars representing SD for in vitro studies or SEM for in vivo studies. Statistical analysis for Fig. 6g was done using a single factor ANOVA.

Results

Ectopic expression of mGluR1 promotes mammary cell proliferation and attenuates luminal apoptosis in 3D morphogenesis

To study the consequences of ectopic mGluR1 expression in mammary epithelial cells, several stable mGluR1-expressing iMMEC (iMMEC-Grm1) clones were generated by transfecting Grm1 cDNA [16] in iMMECs with undetectable levels of endogenous mGluR1 (Fig. 1a). The levels of extracellular glutamate in cultures of iMMEC-Grm1 clones were measured in parallel with MTT cell proliferation/cell viability assays to ensure that any increases in extracellular glutamate were not due to release of intracellular glutamate by cell death. When adjusted for differences in growth rate over the course of the experiment, two independent iMMEC-Grm1 clones showed higher extracellular glutamate levels compared to vector-expressing iMMECs (iMMEC-vector) (Fig. 1b), very similar results to what we and others have shown whereby GPCRs with oncogenic activity such as mGluR1 displayed enhanced levels of locally produced ligands [8, 21].

iMMEC-Grm1 and vector clones were grown on a reconstituted basement membrane in a 3D-cell culture system that promotes the organized development of single-cell acinar structures and mimics ductal morphogenesis occurring during mammary gland development. Oncogenic events perturb this morphogenetic process leading to distorted phenotypes [12, 13].

The induction of apoptosis in central acinar cells during normal mammary morphogenesis was assessed by immunostaining with the activated form of caspase-3, cleaved caspase-3 antibody. β-Catenin stains cell–cell junctions and was used to visualize epithelial cells. In iMMEC-vector acini, apoptosis was visualized in the centrally located cells by day 14 (Fig. 1c). By day 21, we observed the classical formation of a hollow lumen as previously described [10]. Remarkably, forced expression of mGluR1 in two independent iMMEC-Grm1 clones significantly delayed lumen formation, as indicated by the reduced number of apoptotic cells in the luminal space and the quantification of acini exhibiting lumen formation (Fig. 1c).

Next, to determine whether mGluR1 expression affects cellular proliferation during ductal morphogenesis, acinar structures were immunostained with a proliferation marker, Ki-67. Compared to vector-expressing acini, which were mostly hollow, more cells were Ki-67-positive in acini generated by iMMEC-Grm1 clones (Fig. 1d), even within the region of anticipated acinar luminal space.

Ectopic expression of mGluR1 leads to sustained activation of the MAPK/extracellular signal-regulated kinase

Based on our early observations [4, 21] and the hyperactivation of MAPK/ERK in many human neoplasms [22], we investigated the involvement of the MAPK/ERK pathway in mediating the proliferative effects of mGluR1. We probed the acinar structures for the phosphorylated form of ERK and total ERK. At an early time point (Day 7), ERK is highly activated in both vector- and mGluR1-expressing iMMECs (Fig. 2a). This parallels the early events of mammary morphogenesis, which involves robust proliferation before induction of

growth arrest following lumen formation. As expected, we observed a loss of phosphorylated-ERK expression in iMMEC-vector at day 14. In contrast, the signal was continually sustained in iMMEC-Grm1 acini suggesting that mGluR1 may exert its signals in mammary epithelial cells in part through the activated MAPK pathway.

Ectopic expression of mGluR1 perturbs cell polarity

Establishment of apical–basal polarity in mammalian epithelia during mammary morphogenesis is an early event preceding both apoptosis of the central acinar cells and lumen formation [23]. To assess possible polarity changes induced by exogenous mGluR1 expression, we monitored the position of the Golgi apparatus, which is normally oriented toward the acinar lumen. Immunostaining with an apical polarity marker, GM130, showed that iMMEC-Grm1 acini at 21 days post-culture were depolarized and exhibited a disorganized pattern of GM130 staining (Fig. 2b). In contrast, iMMEC-vector acini had a well-developed lumen and polarized Golgi apparatus, suggesting that mGluR1 also affects the ability of mammary epithelial cells to maintain normal polarized organization.

Ectopic expression of mGluR1 induces mammary tumors

The ability to form tumors in in vivo tumorigenicity assays is the ultimate test of oncogenic transformation. To investigate whether glutamatergic signals provided solely by the exogenous expression of mGluR1 in mammary epithelial cells promoted tumorigenesis in vivo, we performed orthotopic implantation of both iMMEC-vector and iMMEC-Grm1 clones into the mammary fat pads of immunodeficient nude mice. The formation of palpable mammary tumors was monitored weekly. iMMEC-Grm1 clones developed mammary tumors as early as 6 weeks post-implantation and a representative figure of the tumor growth kinetics is shown (Fig. 3a, Supplemental Fig. 1). Excised allograft tumors generated by iMMEC-Grm1 clones displayed mGluR1 expression at various levels as demonstrated in immunoblots (Fig. 3b). Interestingly, AKT was activated in the majority of these allograft tumors, but not in the corresponding in vitro cultured iMMECs (Fig. 3b). This observation is similar to our previous report in mGluR1-expressing mouse melanocytic clones [24]. Phosphorylated-ERK levels in the excised tumors were overall stable as shown by the immunoblots (Fig. 3b). Representative high and low magnifications of hematoxylin and eosin (H&E) staining of formalin-fixed sections of the excised allograft tumors are also shown (Fig. 3c). Tumors formed by two independent clones, iMMEC-Grm1-2 and -Grm1-17 displayed a “ribbon and gland” pattern characteristic of moderately differentiated adenocarcinoma with extensive tumor necrosis. Mammary tumors generated by iMMEC-Grm1-18 also showed neoplastic epithelial cells attempting to form glands with an abortive ribbon pattern, that are much less organized than those of iMMEC-Grm1-2 and Grm1-17. Additionally, blood vessels were identified within iMMEC-Grm1-18-generated tumors.

Grm1 suppression leads to phenotypic reversion in vitro and in vivo

To determine whether sustained expression of mGluR1 was required to maintain the observed transformed phenotype, iMMEC-Grm1 clones were engineered to express a tetracycline-inducible siRNA construct targeting Grm1 (siGrm1-iMMECs) or green fluorescent protein (GFP) control (siGFP-iMMECs). Several independent siGrm1-iMMEC clones were isolated and evaluated by immunoblotting. siGrm1-iMMECs demonstrated

consistent suppression of mGluR1 expression in the presence of the inducer, doxycycline (dox), whereas mGluR1 expression remained unchanged in the negative control siGFP clones (Fig. 4a). Next, we assessed if reduced mGluR1 expression modulated cell growth in vitro as measured by the standard MTT cell proliferation/viability assays. Dox-treated siGrm1-iMMEC clones displayed a significant decrease (≈80 %) in the number of viable cells (Fig. 4b). In addition, downregulation of Grm1 in siGrm1-iMMEC-18 rendered these cells less sensitive to an inhibitor of mGluR1 function, riluzole (see below) (Supplemental Fig. 2).

We were also interested in the consequences of reduced mGluR1 levels in 3D acinar morphogenesis. siGrm1-iMMEC clones were grown in 3D culture and at 24 h after plating, doxycycline was added to induce siGrm1 expression. Mammary morphogenesis was assessed after 14 or 21 days of treatment. Consistent with our earlier findings (Fig. 1c), the majority of siGrm1-iMMECs (75 %) formed acini that hollowed centrally when cultured in the presence of doxycycline, whereas much reduced (<30 %) lumen formation was detected in non-dox-induced siGrm1-iMMEC acini (Table 1). Suppression of mGluR1 expression also led to the generation of acini that were approximately 60 % smaller than non-dox-induced siGr-m1-iMMEC clones (Fig. 4c). In acini not treated with doxycycline, similar to our earlier findings (Fig. 1c, d), mGluR1 expression significantly promoted cell proliferation (as assessed by Ki-67 staining) and attenuated apoptosis (as assessed by cleaved caspase-3 staining) (Fig. 4d). In contrast, suppression of Grm1 by siRNA led to reduced number of proliferating cells in the acinar centers and increased levels of apoptotic cells in acinar lumens (Fig. 4d). Inclusion of the siGrm1 inducer, doxycycline, in the culture medium also led to significant attenuation of ERK phosphorylation similar to levels detected in acini formed from vector-expressing iMMECs (Fig. 4d). To ensure that the observed morphology was not an artifact of doxycycline, siGFP-iMMEC clones were subjected to the same 3D-culture conditions and divided into two treatment groups (dox or no treatment). Both groups were analyzed with the same set of antibodies to Ki-67, cleaved caspase-3, and phosphorylated-ERK (Supplemental Fig. 3, Table 1). There were no obvious differences between dox and no treatment groups as both groups exhibited similar patterns of staining as the parental mGluR1-expressing acinar cells.

Next, we assessed by orthotopic allografts whether a reduction of mGluR1 levels modulated iMMEC-Grm1-driven mammary tumorigenesis in vivo. Again, siGrm-iMMEC-18-4 and siGrm-iMMEC-18-8 clones were orthotopically implanted into immunodeficient nude mice. Upon initial appearance of palpable mammary tumors, mice were randomly segregated into two groups with similar tumor volumes and doxycycline was administered in the drinking water of the treated group (0.2 % w/v). Doxycycline-induced Grm1 knockdown suppressed tumor progression of mGluR1-expressing iMMEC allografts, as mammary tumors generated by both siGrm-iMMEC-18-4 and siGrm-iMMEC-18-8 clones in dox-treated mice were about 60 % smaller in volume compared to tumors in the not-treated (NT) mice (Fig. 4e), thus indicating that Grm1 expression is required for the tumorigenic phenotype exhibited by mGluR1-expressing iMMECs in nude mice in vivo.

Grm1 and human breast cancer

mGluR1 is expressed in breast cancer cells and breast cancer tissue biopsies—To investigate the relevance of glutamatergic signaling in human breast cancer, we first extended our studies to breast cancer cell lines. Expression of mGluR1 was detected in several estrogen receptor-positive (ER+) and -negative (ER−) breast cancer cell lines (Fig. 5a). A total of 54 breast cancer cell lines were also analyzed for mGluR1 expression using a gene expression microarray (Supplemental Fig. 4) that showed that a higher percentage of ER-positive breast cancer cell lines (65 %) had greater than average mGluR1 expression as compared to ER-negative lines (35 %).

Next, we compared mGluR1 expression in paired breast tumor to normal adjacent tissue specimens and found that mGluR1 expression in tumors was indeed higher than in normal adjacent tissues, as analyzed by unbiased quantitative assessment of the immunostaining (Fig. 5b). In the adjacent tissue samples, we noticed an interesting pattern of mGluR1 expression localized only to the apical surface of the mammary glands. All three patient samples shown had ER-positive disease.

Possible alterations in the growth properties of ER-positive breast cancer cells by reducing mGluR1 expression were examined. Applying similar approaches to those used for the mouse iMMEC system, we introduced inducible siRNA to GRM1 into mGluR1-expressing MCF7 (siGRM1-MCF7) breast cancer cells (Fig. 5c). In the presence of the inducer, doxycycline, levels of mGluR1 were reduced, as shown by Western immunoblots for two independent siGRM1-MCF7 clones (Fig. 5c) and this suppression of mGluR1 expression decreased the number of viable MCF7 cells in MTT cell proliferation/viability assays (Fig. 5d). Furthermore, the suppression of mGluR1 led to significant decrease in the volume of xenograft tumors generated by MCF7 breast cancer cells, suggesting that mGluR1 signaling is in part required for MCF7 cell proliferation/viability and tumor growth (Fig. 5e).

MCF7 cells respond to the anti-glutamatergic drug riluzole—We had earlier reported elevated levels of extracellular glutamate in cultures of mGluR1-expressing human melanoma cell lines [21]. We examined mGluR1-expressing human breast cancer cell lines and found that both MCF7 and SK-BR-3 secreted higher levels of glutamate as compared to BT474, a non-mGluR1-expressing cell line (Fig. 6a). Our results also confirmed previously published data concerning triple-negative breast cancer cell line, MDA-MB-231 [25], thus indicating that glutamate release and resultant activation of glutamatergic signaling may be frequent occurrences in breast cancer.

In accordance with an important role for Grm1 in melanomagenesis [3], we had previously demonstrated that inhibition of glutamate release by riluzole, an FDA-approved drug for the treatment of amyotrophic lateral sclerosis (ALS), suppressed human melanoma cell growth in vitro and xenograft tumor progression in vivo [21, 26, 27]. In a Phase 0 clinical trial using single agent riluzole for 14 days in patients with resectable stage III/IV melanoma, 34 % of them showed significant decrease in p-AKT and/or p-ERK expression in post-treatment tumor samples, in association with significant decrease in melanoma metabolic activity by FDG-PET [28]. In a Phase II single agent riluzole trial in patients with stages III/IV non-resectable melanoma, the clinical responses were mixed with stable disease, lasting up to

300 days [24]. Three out of the eight available paired pre- and post-treatment tumor samples showed reductions in both p-ERK and p-AKT levels and these were the same patients experiencing stable disease at six-week restaging. Results from the limited set of samples suggest that riluzole has modest anti-tumor activity by itself and more potent glutamatergic inhibitors and/or combinatorial regimens may be more effective in the treatment of melanoma [29]. This was assessed in preclinical combinatorial studies with riluzole and a small molecule AKT inhibitor, MK2206.

First, to determine whether sensitivity of cells to riluzole tracks with the expression of mGluR1, we compared vector-expressing MCF12A to human GRM1-expressing MCF12A cells. We found that exogenous expression of mGluR1 renders the immortalized mammary epithelial cells highly sensitive to riluzole (Fig. 6b). Riluzole inhibited cell proliferation by 20–40 % in three breast cancer cell lines after 96 h, with very small differences observed between 25 and 50 μM, suggesting that 25 μM was sufficient for further studies (Fig. 6c). Furthermore, ER+ MCF7 cells were more sensitive to both mGluR1 antagonist, BAY 36-7620, and riluzole when compared to triple-negative MDA-MB-231 cells (Supplemental Fig. 5). Next, cell cycle profiles were performed on MCF7 and SK-BR-3 cells treated with riluzole for 24 and 48 h. MCF7 cells displayed accumulation at G2/M phase by 24 h and further increase at 48 h (Fig. 6d). MCF7 human breast cancer cells do not express caspase-3 as a result of a 47 base pair deletion within exon 3 of the *casp-3* gene [30]. Despite this, others have shown MCF7 cells to undergo morphological apoptosis after treatment with a variety of agents and under various conditions suggesting caspase-3-independent DNA fragmentation [31, 32]. Indeed, we detected proteolytic processing of PARP in MCF7 cells within 24 h of riluzole treatment (Fig. 6e), despite the lack of accumulation of cells in the sub-G1 phase of the cell cycle (Fig. 6d). For SK-BR-3, first there was a considerable increase in cells accumulating in the G2/M phase at 24 h, followed by an enhanced sub-G1 population after 48 h indicative of cellular apoptosis; a similar observation was reported for human melanoma cells [4, 21].

As with most human cancers, breast tumors are heterogeneous in nature and usually involve multiple oncogenic events occurring in parallel or as part of the same signaling pathway. Given our earlier published results implicating AKT in Grm1-induced melanomagenesis [24, 28] and the well-described role of PI3K/AKT axis in breast cancer pathogenesis and treatment resistance [33], we evaluated the anti-tumor activity of the AKT inhibitor MK-2206 [34] as a single agent and as a possible combinatorial regiment with riluzole. First, we demonstrate that stimulation of mGluR1 with agonist L-Quisqualate leads to activation of both AKT and ERK pathways in MCF7 cells (Fig. 6f). We found that as a single agent only riluzole but not MK-2206 inhibited MCF7 xenograft tumor progression in vivo at a statistical significant level. However, concurrent inhibition of glutamate and AKT signaling using only half the optimal single agent doses resulted in enhanced suppression of tumor growth compared to riluzole alone (Fig. 6g), as calculated by the combination index method [19]. These results indicate that the combination of riluzole and MK-2206 may provide a novel treatment option for patients with ER+ breast cancers.

Discussion

There is mounting evidence that glutamatergic signaling plays a role in epithelial tumorigenesis [5, 7, 8]. In this report, we used a mouse mammary epithelial cell model, involving in vitro 3D-morphogenesis assays and in vivo mammary tumorigenicity studies in nude mice, to examine the tumor-initiating potential of Grm1 in breast cells. Our results demonstrate that ectopic expression of mGluR1 in iMMECs disorganizes 3D acinar architecture and likely promotes cellular transformation, as mGluR1-expressing mammary cells failed to establish hollow and polarized acini as illustrated using staining patterns and marker antibodies (Fig. 1 and Supplemental Fig. 6). Furthermore, mGluR1 expression in iMMECs was sufficient to promote moderately to poorly differentiated tumor development in a system of very low inherent tumorigenic potential [10]. In support of a driving role for Grm1 in mammary tumorigenesis, Grm1 knockdown by an inducible siRNA system suppressed iMMEC-Grm1 cell proliferation in vitro and allograft mammary tumor progression in vivo. In addition, using similar approaches in mGluR1- and ER-expressing MCF7 human breast cancer cells, we also observed comparable results to those obtained with the mouse mammary epithelial cell system.

mGluR1 is a member of the seven transmembrane G-protein-coupled receptor (GPCR) superfamily, which represents a potent group of highly druggable targets encompassing approximately more than a quarter of all FDA-approved drugs [35]. Found in abundance in post-synaptic locations, mGluR1 is activated by its natural ligand, the major neurotransmitter L-glutamate and was first thought to be functionally restricted to the central nervous system. However, mGluR1 expression has recently been demonstrated in peripheral tissues. The notion that wild-type GPCRs may harbor oncogenic potential is not entirely surprising. This concept underscores several key characteristics of a tumorigenic GPCR, such as aberrant expression or response to excessive locally circulating ligand produced by the tumor or neighboring cells [36]. Autocrine and/or possibly paracrine loops have been described for mGluR1-expressing human melanoma cells [21]. It is also well established that glioma cells release excessive glutamate not only to enhance cell motility and invasion, but also to aid in the expansion of tumor cells through its excitotoxicity effects [37]. Interestingly, triple-negative MDA-MB-231 breast cancer cells have been reported to release extracellular glutamate, which may function as a cytokine that promotes bone invasion, thus enhancing metastasis [25]. Here we demonstrate that ectopic mGluR1 expression in estrogen receptor-positive iMMECs results in amplified release of extracellular glutamate consistent with our previous studies in melanoma [4, 38].

In this paper, we also report that introduction of exogenous Grm1 in a mouse mammary epithelial cell model system leads to altered cell growth characteristics, including increased proliferation and suppression of central mammary cell apoptosis resulting in larger acini and delayed lumen formation in 3D morphogenesis assays. Using phosphorylated-ERK levels as read-outs, we found that mGluR1 activates MAP Kinase (MAPK), a pathway that regulates cell proliferation and is often deregulated in cancer. At day 7 post-plating in 3D cultures, both vector- and mGluR1-expressing iMMEC clones exhibited similar levels of activated ERK, presumably due to the early proliferative spheroid organization step in mammary morphogenesis. However, by day 14, phospho-ERK levels were essentially undetectable in

acini, generated by vector-but were still detectable in mGluR1-expressing iMMECs. Indeed, components of the MAPK pathway have been shown to not only regulate proliferation signals in mammary epithelial cells, but also function in the control of cell survival by regulating the activity of proapoptotic molecules, such as Bim [39, 40]. We have previously shown that mGluR1 supports cell survival through activation of the PI3K/AKT pathway in Grm1-transformed mouse melanocytic clones and that AKT2 knockdown by siRNA in these cells leads to apparent reduction in the levels of the anti-apoptotic protein, BCL2 [24, 41]. Interestingly, in the current study, we also detected stimulation of AKT in excised tumors generated by mGluR1-expressing iMMECs in nude mice in vivo, but not in the same cells under normal culture conditions in vitro (Fig. 3b). Speyer and colleagues also detected activated AKT only when the cultured cells were stimulated with mGluR1 agonist, L-Quisqualate [5]. Taken together, these results suggest that activation of the PI3K/AKT axis may require stimulation of the receptor mGluR1 by its agonist in vitro or in an in vivo ligand-rich microenvironment.

There are many advantages to employing 3D culture systems, especially in studies of glandular epithelium such as that of the mammary gland, as compared to traditional 2D cell cultures. These 3D systems allow a distinction between non-malignant and malignant cells by various phenotypic alterations. Non-transformed cells usually form polarized, growth-arrested acini-like spheroids in the presence of laminin-rich extracellular matrix, while transformed cells may exhibit perturbed lumen formation, polarity, and acinar structure and size [10, 11, 13]. We now present such findings in mGluR1-expressing iMMECs, which generate larger, non-hollowing, and non-polarized acini exhibiting increased cell proliferation and persistent ERK activation. Interestingly, cell proliferation, as measured by MTT cell viability assays, was modestly affected by mGluR1 expression in iMMECs plated in 2D cultures (Supplemental Fig. 7), thus, suggesting that cell–cell interactions in a more physiologically relevant 3D context are crucial for Grm1 to exert its transformative effects in mammary epithelial cells. Moreover, we were also able to regulate mGluR1 expression in iMMEC-Grm1 clones by an inducible silencing RNA system to Grm1, where a reduction in mGluR1 expression levels correlated with phenotypic reversion in 3D cultures. Notably, we demonstrated that orthotopic implantation of mGluR1-expressing iMMECs into the mammary fat pads of athymic mice was sufficient and also required to promote robust tumor formation, thus supporting the idea that Grm1 may be an important player in mammary tumorigenesis.

We investigated the consequences of GRM1 modulation in MCF7, a breast cancer cell line belonging to the luminal A subtype. Patients with hormone receptor (ER)-positive luminal A tumors have better prognosis, as such malignancies usually respond to estrogen deprivation; however, about half of the patients with advanced ER-positive disease show resistance to hormonal intervention. In a recently published study [6], 17β-estradiol increased the expression of mGluR1 in MCF7 cells and this increase was inhibited by pre-treatment with a selective estrogen receptor modulator, 4-hydroxytamoxifen suggesting a novel interaction between mGluR1 and hormone signaling. Importantly, a polymorphic variant of GRM1 was shown to be associated with risk for luminal breast cancer and mGluR1 expression correlated with decreased survival in tamoxifen-treated patients [6]. It is of great interest that, unlike the widely used MCF10A human mammary epithelial cells, iMMECs are

estrogen receptor α-expressing cells [13]. Whether Grm1-mediated transformation of iMMECs is dependent on ER is a provocative question and is currently being investigated.

Taken together, our findings provide evidence that aberrant glutamate signaling can initiate transformation and tumorigenic properties in normal mammary epithelial cells. Based on our results and in agreement with two recent reports [5, 6], we propose that modulation of glutamatergic signaling alone or in combination with other small molecule inhibitors such as MK-2206 may offer therapeutic benefits to patients with either luminal or basal subtype of the disease. A proposed model depicts possible involvement of glutamate signaling in mammary pathogenesis (Fig. 6h). Key questions regarding the regulation of mGluR1 in breast tissues and breast cancer cells will be the focus of future investigations and may lead to new diagnostic and therapeutic opportunities.

Supplementary Material

Refer to Web version on PubMed Central for supplementary material.

Acknowledgments

This work was supported by grants NIH-NCI R00 and Damon Runyon Clinical Investigator Award to V.K. and Biospecimen Repository Service, and Histopathology and Imaging Shared Resources of Rutgers Cancer Institute of New Jersey (P30CA072720) to K.H. The authors would like to thank Dr. Brian Wall for assisting in our animal experiments. We would also like to acknowledge the generosity of Merck & Co., Inc. and the National Cancer Institute, National Institutes of Health for the MK-2206 drug, Dr. Nanjoo Suh (Rutgers University, Piscataway, NJ, USA) for the human breast cancer cell lines, Dr. Tony Kong (Rutgers University, Piscataway, NJ, USA) for Aperio digital slide scanning/quantification system access, Dr. Carol Gardner and Dr. Debra Laskin for Olympus BX51 microscope and camera access, and Dr. Renping Zhou for Nikon D-Eclipse C1 confocal microscope system access.

References

1. Prickett TD, Wei X, Cardenas-Navia I, Teer JK, Lin JC, Walia V, et al. Exon capture analysis of G protein-coupled receptors identifies activating mutations in GRM3 in melanoma. Nat Genet. 2011; 43(11):1119–1126. (Epub 2011/09/29). [PubMed: 21946352]
2. Wei X, Walia V, Lin JC, Teer JK, Prickett TD, Gartner J, et al. Exome sequencing identifies GRIN2A as frequently mutated in melanoma. Nat Genet. 2011; 43(5):442–446. (Epub 2011/04/19). [PubMed: 21499247]
3. Pollock PM, Cohen-Solal K, Sood R, Namkoong J, Martino JJ, Koganti A, et al. Melanoma mouse model implicates metabotropic glutamate signaling in melanocytic neoplasia. Nat Genet. 2003; 34(1):108–112. (Epub 2003/04/22). [PubMed: 12704387]
4. Shin SS, Namkoong J, Wall BA, Gleason R, Lee HJ, Chen S. Oncogenic activities of metabotropic glutamate receptor 1 (Grm1) in melanocyte transformation. Pigment Cell Melanoma Res. 2008; 21(3):368–378. (Epub 2008/04/26). [PubMed: 18435704]
5. Speyer CL, Smith JS, Banda M, Devries JA, Mekani T, Gorski DH. Metabotropic glutamate receptor-1: a potential therapeutic target for the treatment of breast cancer. Breast Cancer Res Treat. 2011; 132(2):565–573. (Epub 2011/06/18). [PubMed: 21681448]
6. Mehta MS, Dolfi SC, Bronfenbrener R, Bilal E, Chen C, Moore D, et al. Metabotropic glutamate receptor 1 expression and its polymorphic variants associate with breast cancer phenotypes. PLoS One. 2013; 8(7):e69851. (Epub 2013/08/08). [PubMed: 23922822]
7. Koochekpour S, Majumdar S, Azabdaftari G, Attwood K, Scioneaux R, Subramani D, et al. Serum glutamate levels correlate with Gleason score and glutamate blockade decreases proliferation, migration, and invasion and induces apoptosis in prostate cancer cells. Clin Cancer Res. 2012; 18(21):5888–5901. (Epub 2012/10/18). [PubMed: 23072969]

8. Martino JJ, Wall BA, Mastrantoni E, Wilimczyk BJ, La Cava SN, Degenhardt K, et al. Metabotropic glutamate receptor 1 (Grm1) is an oncogene in epithelial cells. Oncogene. 2012 (Epub 2012/10/23).
9. Siegel R, Naishadham D, Jemal A. Cancer statistics, 2013. CA Cancer J Clin. 2013; 63(1):11–30. (Epub 2013/01/22). [PubMed: 23335087]
10. Karantza-Wadsworth V, White E. A mouse mammary epithelial cell model to identify molecular mechanisms regulating breast cancer progression. Methods Enzymol. 2008; 446:61–76. (Epub 2008/07/08). [PubMed: 18603116]
11. Debnath J, Muthuswamy SK, Brugge JS. Morphogenesis and oncogenesis of MCF-10A mammary epithelial acini grown in three-dimensional basement membrane cultures. Methods. 2003; 30(3): 256–268. (Epub 2003/06/12). [PubMed: 12798140]
12. Liu Y, Chen N, Cui X, Zheng X, Deng L, Price S, et al. The protein kinase Pak4 disrupts mammary acinar architecture and promotes mammary tumorigenesis. Oncogene. 2010; 29(44):5883–5894. (Epub 2010/08/11). [PubMed: 20697354]
13. Karantza-Wadsworth V, Patel S, Kravchuk O, Chen G, Mathew R, Jin S, et al. Autophagy mitigates metabolic stress and genome damage in mammary tumorigenesis. Genes Dev. 2007; 21(13):1621–1635. (Epub 2007/07/04). [PubMed: 17606641]
14. Cohen-Solal KA, Crespo-Carbone SM, Namkoong J, Mackason KR, Roberts KG, Reuhl KR, et al. Progressive appearance of pigmentation in amelanotic melanoma lesions. Pigment Cell Res. 2002; 15(4):282–289. (Epub 2002/07/09). [PubMed: 12100494]
15. Degenhardt K, White E. A mouse model system to genetically dissect the molecular mechanisms regulating tumorigenesis. Clin Cancer Res. 2006; 12(18):5298–5304. (Epub 2006/09/27). [PubMed: 17000662]
16. Zhu H, Ryan K, Chen S. Cloning of novel splice variants of mouse mGluR1. Brain Res Mol Brain Res. 1999; 73(1–2):93–103. [PubMed: 10581402]
17. Stepulak A, Sifringer M, Rzeski W, Endesfelder S, Gratopp A, Pohl EE, et al. NMDA antagonist inhibits the extracellular signal-regulated kinase pathway and suppresses cancer growth. Proc Natl Acad Sci USA. 2005; 102(43):15605–15610. (Epub 2005/10/19). [PubMed: 16230611]
18. Wu TY, Saw CL, Khor TO, Pung D, Boyanapalli SS, Kong AN. In vivo pharmacodynamics of indole-3-carbinol in the inhibition of prostate cancer in transgenic adenocarcinoma of mouse prostate (TRAMP) mice: involvement of Nrf2 and cell cycle/apoptosis signaling pathways. Mol Carcinog. 2012; 51(10):761–770. (Epub 2011/08/13). [PubMed: 21837756]
19. Zhang Y, Song S, Yang F, Au JL, Wientjes MG. Nontoxic doses of suramin enhance activity of doxorubicin in prostate tumors. J Pharmacol Exp Ther. 2001; 299(2):426–433. (Epub 2001/10/17). [PubMed: 11602651]
20. Neve RM, Chin K, Fridlyand J, Yeh J, Baehner FL, Fevr T, et al. A collection of breast cancer cell lines for the study of functionally distinct cancer subtypes. Cancer Cell. 2006; 10(6):515–527. (Epub 2006/12/13). [PubMed: 17157791]
21. Namkoong J, Shin SS, Lee HJ, Marin YE, Wall BA, Goydos JS, et al. Metabotropic glutamate receptor 1 and glutamate signaling in human melanoma. Cancer Res. 2007; 67(5):2298–2305. (Epub 2007/03/03). [PubMed: 17332361]
22. Dhillon AS, Hagan S, Rath O, Kolch W. MAP kinase signalling pathways in cancer. Oncogene. 2007; 26(22):3279–3290. (Epub 2007/05/15). [PubMed: 17496922]
23. Debnath J, Mills KR, Collins NL, Reginato MJ, Muthuswamy SK, Brugge JS. The role of apoptosis in creating and maintaining luminal space within normal and oncogene-expressing mammary acini. Cell. 2002; 111(1):29–40. (Epub 2002/10/10). [PubMed: 12372298]
24. Shin SS, Wall BA, Goydos JS, Chen S. AKT2 is a downstream target of metabotropic glutamate receptor 1 (Grm1). Pigment Cell Melanoma Res. 2010; 23(1):103–111. (Epub 2009/10/22). [PubMed: 19843246]
25. Seidlitz EP, Sharma MK, Saikali Z, Ghert M, Singh G. Cancer cell lines release glutamate into the extracellular environment. Clin Exp Metastasis. 2009; 26(7):781–787. (Epub 2009/06/16). [PubMed: 19526315]
26. Khan AJ, Wall B, Ahlawat S, Green C, Schiff D, Mehnert JM, et al. Riluzole enhances ionizing radiation-induced cytotoxicity in human melanoma cells that ectopically express metabotropic

glutamate receptor 1 in vitro and in vivo. Clin Cancer Res. 2011; 17(7):1807–1814. (Epub 2011/02/18). [PubMed: 21325066]

27. Lee HJ, Wall BA, Wangari-Talbot J, Shin SS, Rosenberg S, Chan JL, et al. Glutamatergic pathway targeting in melanoma: single-agent and combinatorial therapies. Clin Cancer Res. 2011; 17(22): 7080–7092. (Epub 2011/08/17). [PubMed: 21844014]
28. Yip D, Le MN, Chan JL, Lee JH, Mehnert JA, Yudd A, et al. A phase 0 trial of riluzole in patients with resectable stage III and IV melanoma. Clin Cancer Res. 2009; 15(11):3896–3902. (Epub 2009/05/22). [PubMed: 19458050]
29. Mehnert JMWY, Lee JH, Jeong BS, Li J, Dudek Pruski-Clark LL, Kane MM, Lin H, Shih W, Chen S, Goydos JS. A phase II trial of riluzole, an antagonist of metabotropic glutamate receptor 1 (GRM1) signaling, in patients with advanced melanoma. 2013 (Submitted).
30. Janicke RU, Sprengart ML, Wati MR, Porter AG. Caspase-3 is required for DNA fragmentation and morphological changes associated with apoptosis. J Biol Chem. 1998; 273(16):9357–9360. (Epub 1998/05/23). [PubMed: 9545256]
31. Mooney LM, Al-Sakkaf KA, Brown BL, Dobson PR. Apoptotic mechanisms in T47D and MCF-7 human breast cancer cells. Br J Cancer. 2002; 87(8):909–917. (Epub 2002/10/10). [PubMed: 12373608]
32. McGee MM, Hyland E, Campiani G, Ramunno A, Nacci V, Zisterer DM. Caspase-3 is not essential for DNA fragmentation in MCF-7 cells during apoptosis induced by the pyrrolo-1,5-benzoxazepine, PBOX-6. FEBS Lett. 2002; 515(1–3):66–70. (Epub 2002/04/12). [PubMed: 11943196]
33. Tokunaga E, Kimura Y, Mashino K, Oki E, Kataoka A, Ohno S, et al. Activation of PI3K/Akt signaling and hormone resistance in breast cancer. Breast Cancer. 2006; 13(2):137–144. (Epub 2006/06/07). [PubMed: 16755107]
34. Hirai H, Sootome H, Nakatsuru Y, Miyama K, Taguchi S, Tsujioka K, et al. MK-2206, an allosteric Akt inhibitor, enhances antitumor efficacy by standard chemotherapeutic agents or molecular targeted drugs in vitro and in vivo. Mol Cancer Ther. 2010; 9(7):1956–1967. (Epub 2010/06/24). [PubMed: 20571069]
35. Overington JP, Al-Lazikani B, Hopkins AL. How many drug targets are there? Nat Rev Drug Discov. 2006; 5(12):993–996. (Epub 2006/12/02). [PubMed: 17139284]
36. Dorsam RT, Gutkind JS. G-protein-coupled receptors and cancer. Nat Rev Cancer. 2007; 7(2):79–94. (Epub 2007/01/26). [PubMed: 17251915]
37. de Groot J, Sontheimer H. Glutamate and the biology of gliomas. Glia. 2011; 59(8):1181–1189. (Epub 2010/12/31). [PubMed: 21192095]
38. Lee HJ, Wall BA, Wangari-Talbot J, Shin SS, Rosenberg SA, Chan JL, et al. Glutamatergic pathway targeting in melanoma; single agent and combinatorial therapies. Clin Cancer Res. 2011; 17(22):7080–7092. (Epub 2011/08/17). [PubMed: 21844014]
39. Marani M, Hancock D, Lopes R, Tenev T, Downward J, Lemoine NR. Role of Bim in the survival pathway induced by Raf in epithelial cells. Oncogene. 2004; 23(14):2431–2441. (Epub 2003/12/17). [PubMed: 14676826]
40. Reginato MJ, Mills KR, Becker EB, Lynch DK, Bonni A, Muthuswamy SK, et al. Bim regulation of lumen formation in cultured mammary epithelial acini is targeted by oncogenes. Mol Cell Biol. 2005; 25(11):4591–4601. (Epub 2005/05/19). [PubMed: 15899862]
41. Teh JL, Shah R, Shin SS, Wen Y, Mehnert J, Goydos J, Chen S. Metabotropic glutamate receptor 1 mediates melanocyte transformation via transactivation of insulin-like growth factor 1 receptor. Pigment Cell Res. 2014; 27(4):621–629.

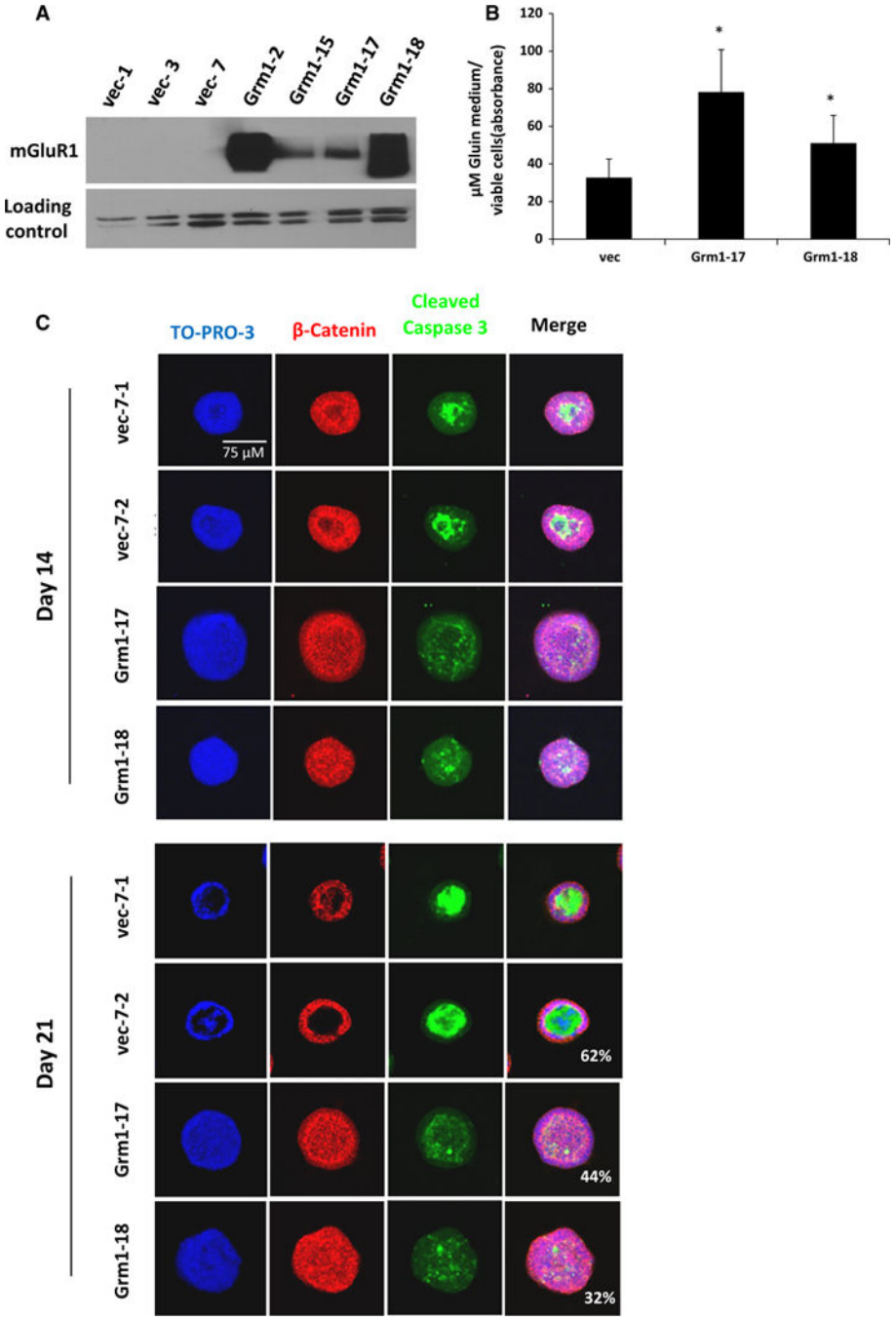

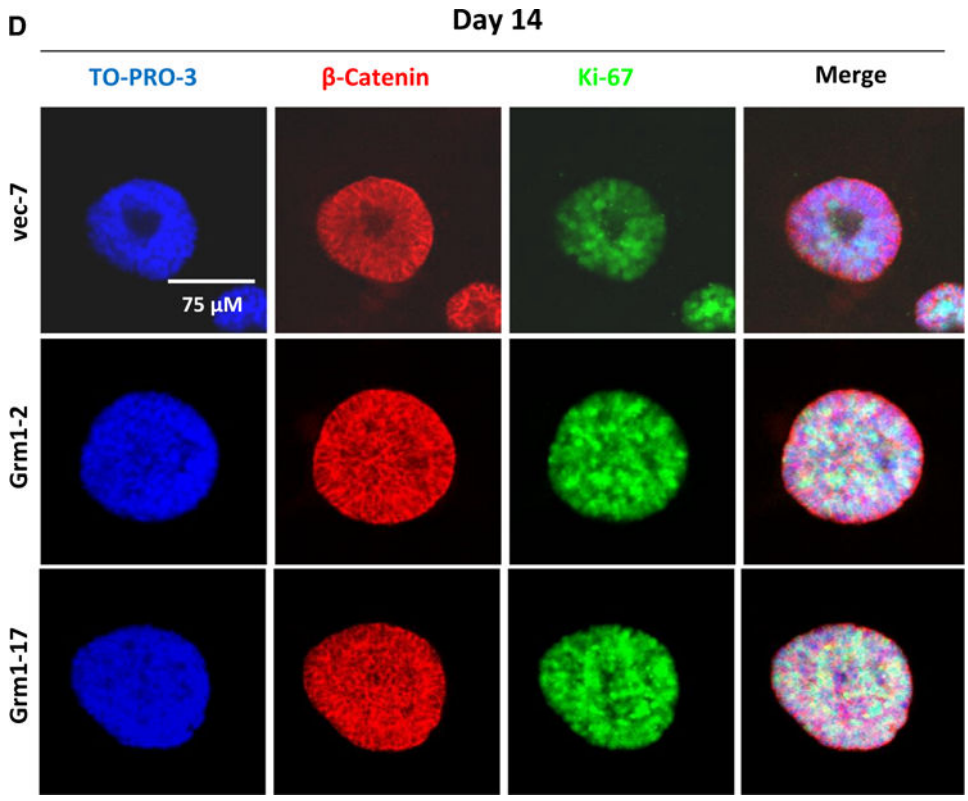

Fig. 1.

mGluR1 reduces apoptosis and promotes proliferation in iMMEC-Grm1 clones. **a** Expression of mGluR1 in iMMECs after transfection with a full-length Grm1 α-form in pCI-neo or empty vector pCI-neo alone (vec). Independent stable clones exhibited varying levels of mGluR1 expression shown by immunoblotting. Total ERK was used as loading control. **b** iMMEC-Grm1 clones release glutamate. At the time of measurement (Day 4), half the volume of medium was removed for glutamate assay and the other half for cell viability assessed by MTT. iMMEC-Grm1 clones released increased levels of extracellular glutamate when compared to iMMEC-vector even when adjusted for difference in growth rate as measured by MTT (*$P < 0.05$, *t*-test, *error bars* represent SD). **c** Inhibition of apoptosis in iMMEC-Grm1. iMMECs stably expressing either empty vector (vec-7) or mGluR1 were grown in 3D cultures. Acini were stained with TO-PRO 3 (*blue* for nuclear counterstaining), β-catenin (*red* to visualize epithelial cells), and cleaved caspase-3 (*green* as an apoptosis marker). Images are shown for acinar morphology at day 14 and 21 after plating. Images are representative of the majority of acini for a specific genotype at a given time point. Two representative images are shown for vector (vec-7-1 and vec-7-2). The number indicated at the bottom right corner is the percentage of acini with lumen formation. A total of 300 acinar structures were evaluated for lumen formation. **d** Ectopic expression of mGluR1 promotes proliferation in iMMECs. Ki-67 (*green*) is used to visualize proliferating cells, TO-PRO 3 (*blue* for nuclear counterstaining) and β-catenin (*red* to visualize epithelial cells). Proliferating cells could be seen in the lumens of acini generated by mGluR1-expressing iMMECs, whereas Ki-67 signals were reduced or absent in the lumens of vec-7 acini

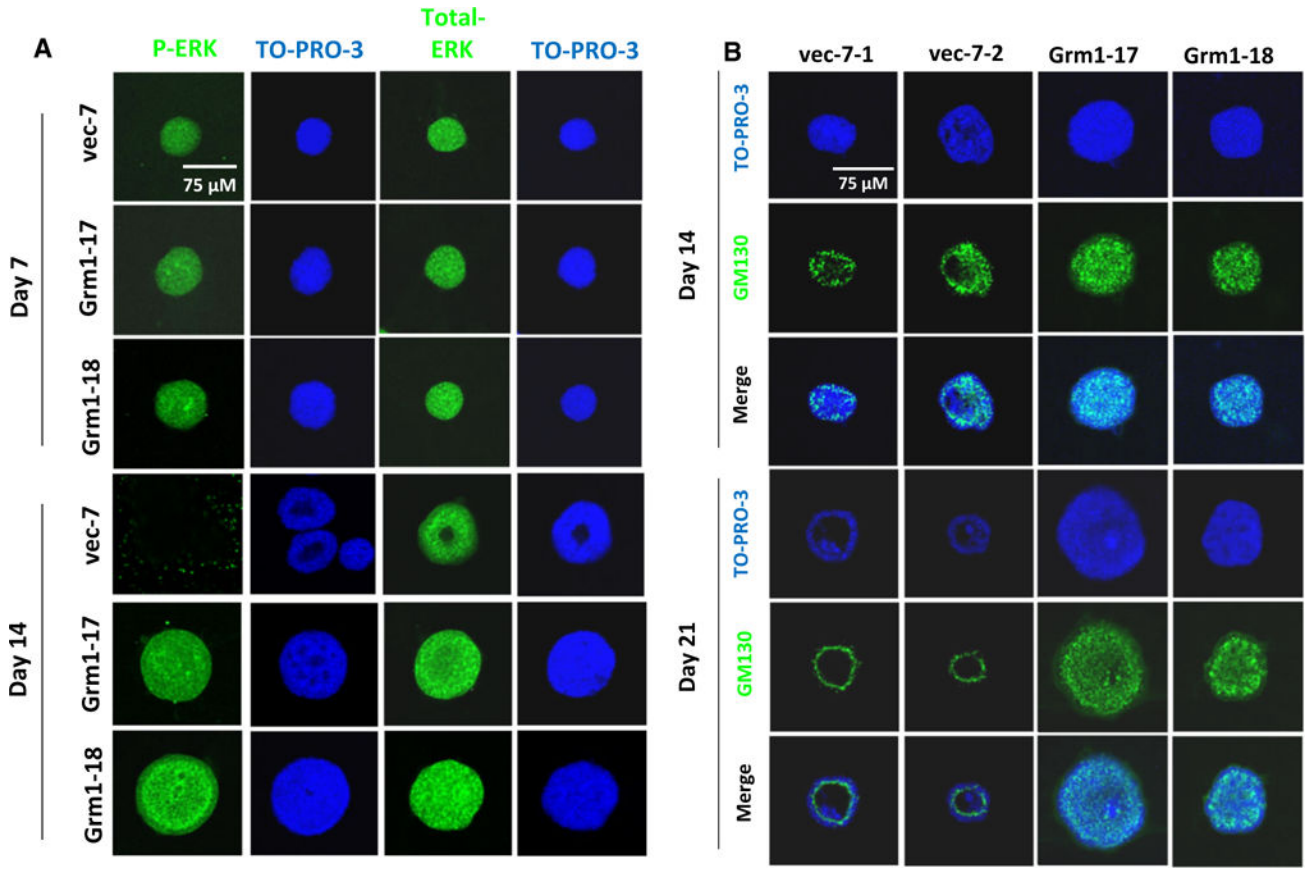

Fig. 2.

Ectopic expression of mGluR1 sustains ERK activation and disrupts cell polarity. **a** iMMECs-expressing empty vector clone (vec-7) or two independent mGluR1-expressing iMMEC clones (Grm1-17 and Grm1-18) were plated in 3D culture. At days 7 and 14 after plating, acini were immunostained for phosphorylated-ERK or total ERK (*green*) to visualize ERK activation; nuclei were visualized by TO-PRO-3 (*blue*). At day 7, phosphorylated-ERK levels were similar in all clones, but at day 14, phosphorylated-ERK staining was absent in vec-7, but still very prominent in two mGluR1-expressing iMMEC clones. Total ERK levels were similar in all clones. **b** Ectopic expression of mGluR1 induces disruption in cell polarity. Acini are shown at day 14 and day 21 after plating in 3D culture. Two representative images are shown for vector (vec-7-1 and vec-7-2). GM130 (*green*), a cell polarity marker, stains the apical orientation of the Golgi apparatus toward the lumen of the acini. TO-PRO-3 (*blue*) is utilized to visualize nuclei of all cells

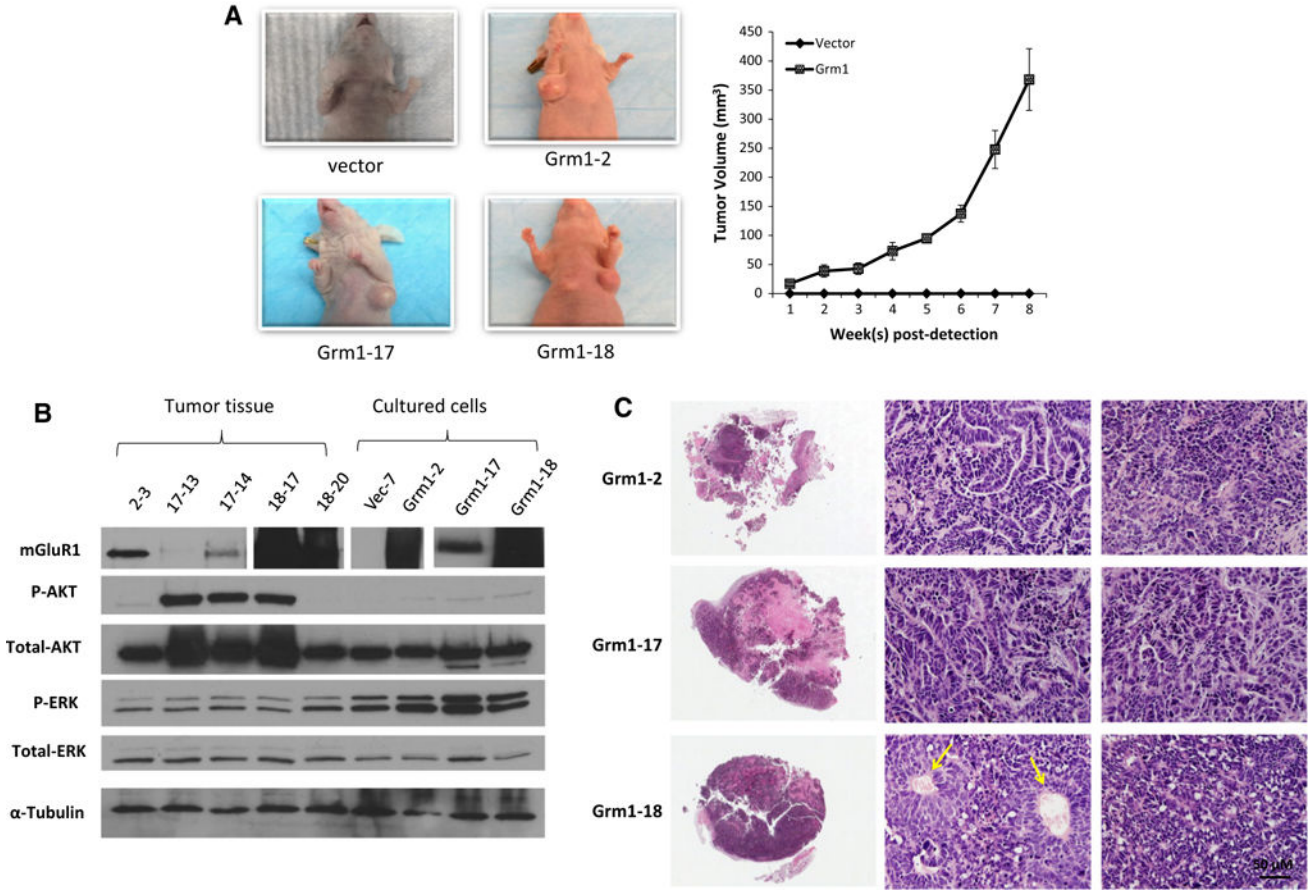

Fig. 3.

mGluR1 ectopically expressed in iMMECs promotes mammary tumor formation in athymic nude mice. **a** At 6 weeks after orthotopic implantation of iMMEC-Grm1 cells, palpable tumors were detected. All three iMMEC-Grm1 clones tested were tumorigenic in vivo (*left panel*). A representative graph of allograft tumor growth kinetics is shown (*right panel*) (vector clones; $n = 5$, iMMEC-Grm1 clones; $n = 15$, 5 mice peer clone, *error bars* represent SEM). **b** Levels of mGluR1, phosphorylated-AKT, and phosphorylated-ERK in cultured iMMEC-Grm1 clones and corresponding allograft tumors were examined by Western immunoblots. mGluR1 expression was detected in cultured cells and excised tumors; various levels of phosphorylated-ERK were observed in all samples; phosphorylated-AKT was detected only in excised allograft tumors, but not in iMMEC-Grm1 cells in regular 2D culture. **c** Two representative images of H&E staining of tumors generated by iMMEC-Grm1 clones (*left panel*, 100× magnification, *middle* and *right* panel, 400× magnification). *Arrows* point to blood vessels identified within iMMEC-Grm1 tumor

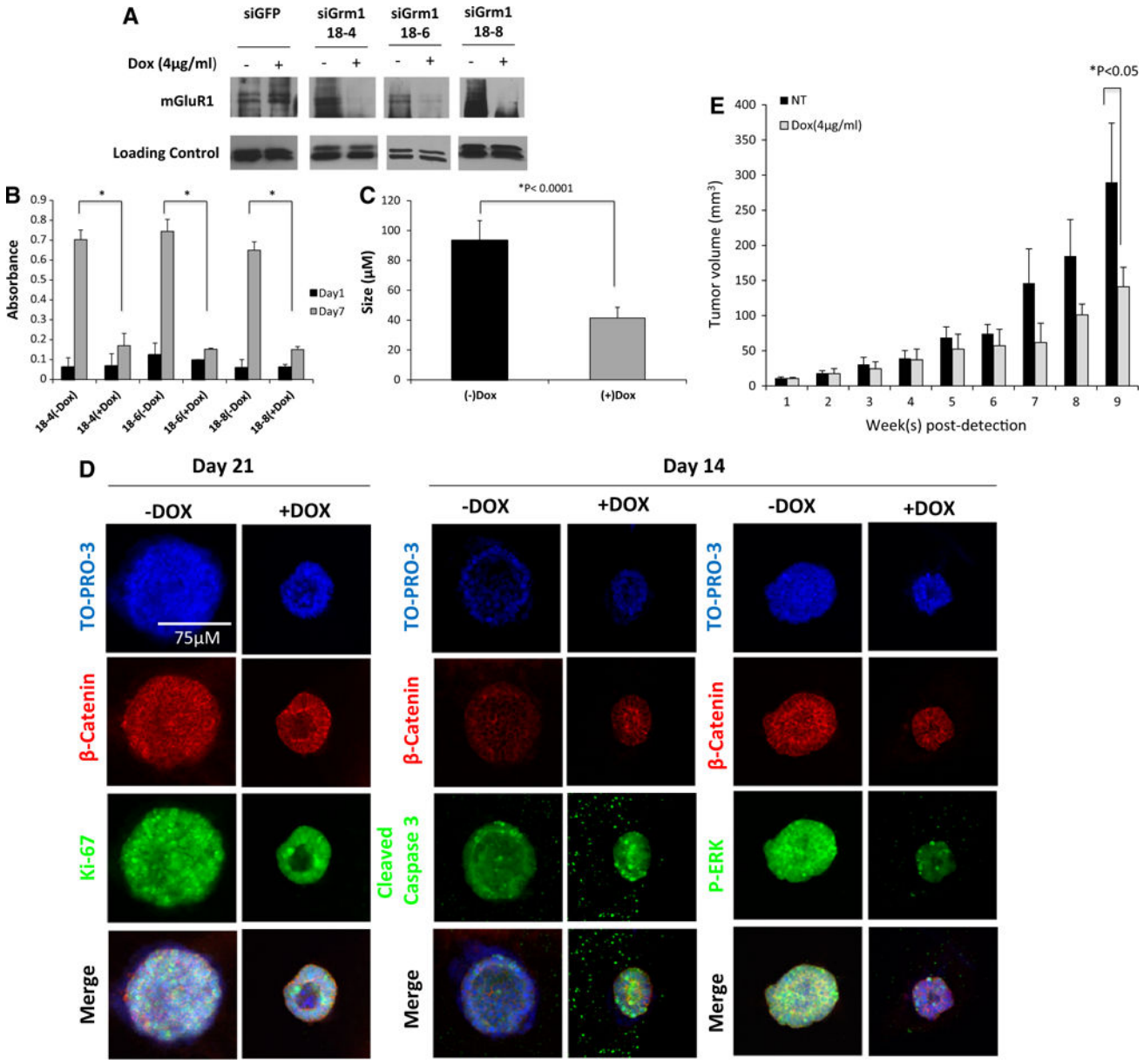

Fig. 4.

Sustained mGluR1 expression is required to maintain transformed phenotypes. **a** Several independent clones were isolated from introduction of inducible siRNA to GFP (control) or Grm1 in mGluR1-expressing iMMECs. In the presence of the inducer, doxycycline, mGluR1 expression was reduced at the protein level as assessed by immunoblots only in siGrm1-iMMEC, but not siGFP-iMMEC clones. Total ERK was used as loading control. **b** MTT cell viability/proliferation assays were performed in the same set of cells and a decrease in the number of viable cells was detected only in the presence of doxycycline (*$P < 0.0002$, *t*-test, *error bars* represent SD, for dox treatment versus no treatment). **c** The size of siGrm1-iMMEC acini was measured on day 14, following treatment with doxycycline (4 μg/ml) and compared to not-treated acini (*$P < 0.0001$, *t*-test, *error bars* represent SD). **d** Knockdown of mGluR1 expression by siRNA led to phenotypic reversion of iMMEC-Grm1

clones at day 14 or 21 after treatment with doxycycline (4 μg/ml) in 3D cultures. Acini were immunostained for Ki-67, cleaved caspase-3, phosphorylated-ERK, and β-catenin to visualize epithelial cells and TO-PRO-3 to visualize nuclei. **e** In vivo suppression of tumor progression by siGrm1. Mice bearing mammary tumors generated from siGrm1-iMMEC cells were treated with doxycycline (0.2 % w/v in drinking water) to induce expression of siRNA to Grm1. Results indicate that sustained expression of Grm1 is partially necessary to maintain iMMEC-Grm1 tumor progression, (*$P < 0.05$, *t* test, $n = 5$ in each group, *error bars* represent SEM). Not-treated siGrm1-iMMEC allografts progressed with similar growth kinetics as tumors generated by iMMEC-Grm1 cells

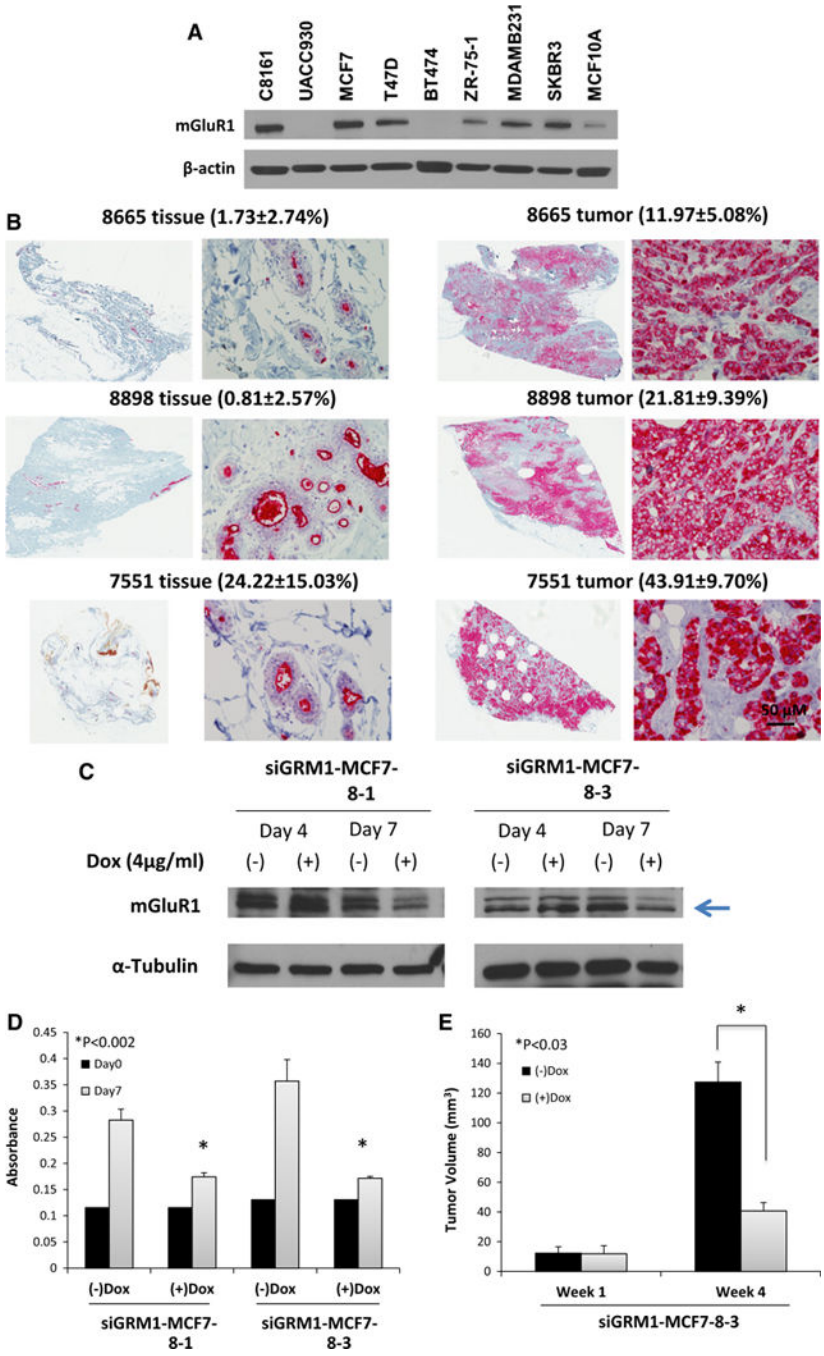

Fig. 5.

mGluR1 is overexpressed in breast cancer cell lines and tumor tissues. **a** mGluR1 expression by Western blot in melanoma cell lines C8161, UACC930 (positive and negative control, respectively); breast cancer cell lines MCF7, T47D, BT-474, and ZR-75-1 [ER+]; SK-BR-3 [ER−, HER2+]; MDA-MB-231 [triple-negative], MCF10A [immortalized human ER− mammary epithelial cells]. **b** IHC for mGluR1 in paired breast tumor(T) and adjacent normal (N) biopsies. mGluR1-positive cells (% of total cells) scored in each digitized slide by an unbiased quantitative assessment using Aperio ScanScopeGL and ImageScope

software. Photomicrographs of IHC, representative paired tissue Sects. ×100 and ×400 magnification. **c** Inducible siGRM1 constructs were introduced into MCF7 breast cancer cells; several independent clones were isolated and characterized. In the presence of doxycycline, endogenous mGluR1 levels were reduced as assessed by immunoblots. **d** Reduction of viable cell numbers when siGRM1-MCF7 cells were treated with doxycycline, $*P < 0.002$, *t* test, *error bars* represent SD, for both clones, comparing dox treatment versus no treatment. **e** Inducible siRNA to GRM1 reduced progression of xenograft tumors generated by orthotopic implantation of MCF7 breast cancer cells ($*P < 0.03$, *t* test, $n = 6$ in each group, *error bars* represent SEM)

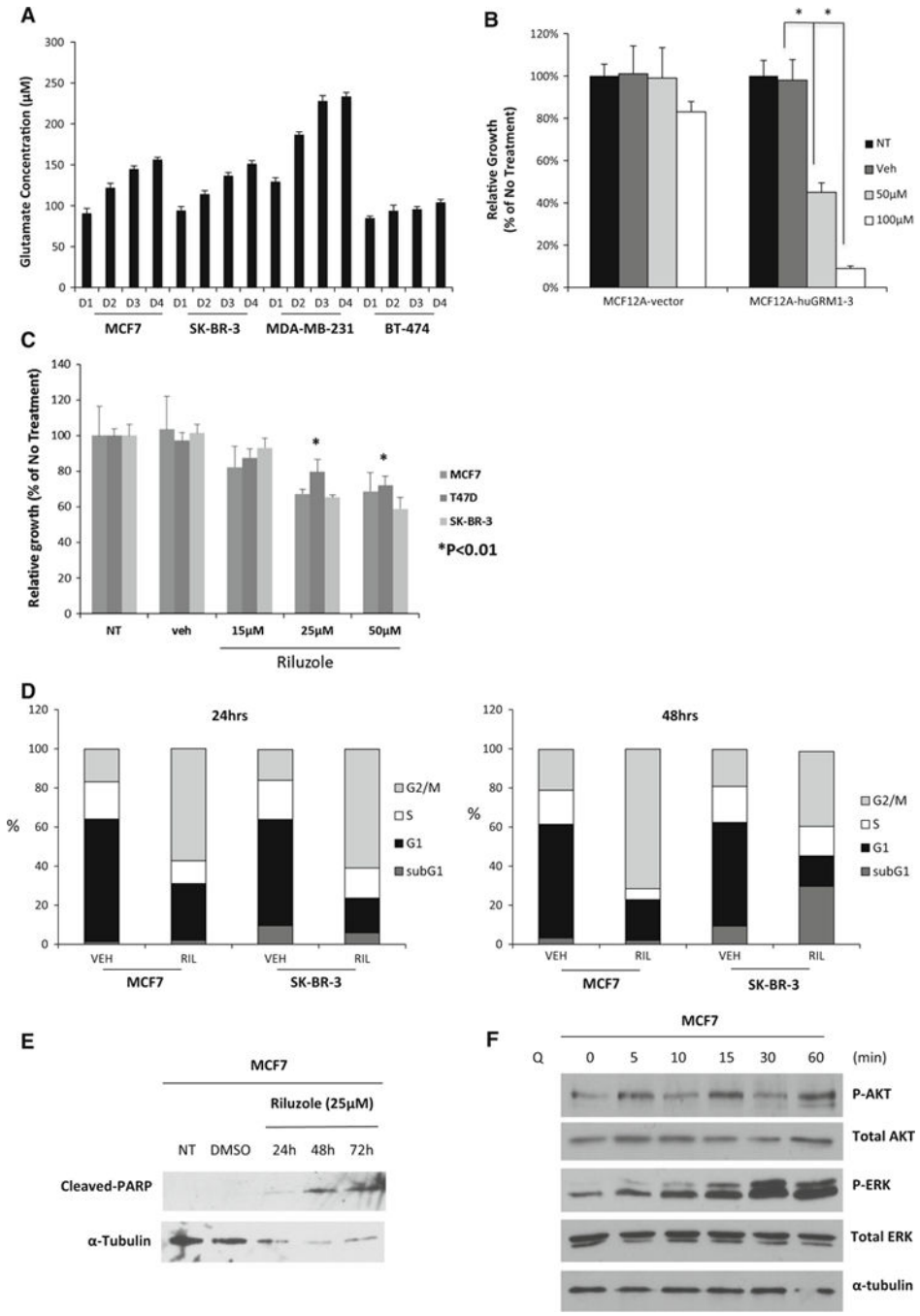

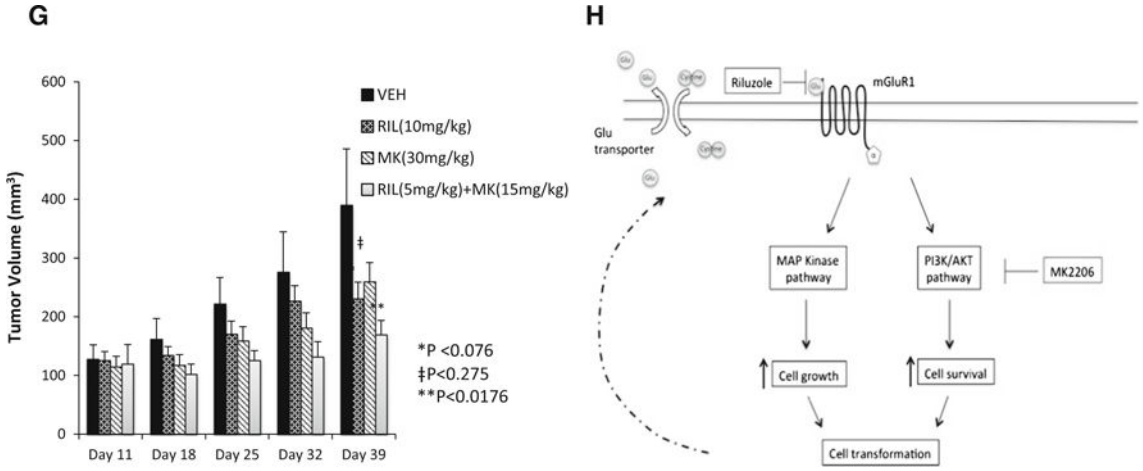

Fig. 6.

Anti-glutamatergic drug riluzole modulates ER-positive andc ER-negative breast cancer cell growth. **a** mGluR1-expressing breast cancer cells release excessive extracellular glutamate. **b** MTT cell viability assay of MCF12A-vector and MCF12A-huGRM1 cells treated with riluzole for 5 days (**P* < 0.0005, *t* test, *error bars* represent SD). **c** MTT cell proliferation viability assays were performed with three human breast cancer cell lines treated with riluzole for 96 h. All three lines exhibited reduced cell proliferation in the presence of riluzole (**P* < 0.01, *t* test, *error bars* represent SD). **d** Cell cycle profiles of two human breast cancer cell lines: MCF7 and SK-BR-3 cells displayed apparent cytostatic and cytotoxic responses, respectively, in the presence of riluzole. **e** Elevated levels of PARP cleavage in MCF7 cells treated with riluzole. NT (no treatment) at 72 h, DMSO (vehicle) at 72 h, riluzole at 24, 48, and 72 h. **f** Induction of mGluR1 with L-Quisqualate activates ERK and AKT in MCF7 cells. **g** In vivo reduction of tumor progression by the combination of riluzole and AKT inhibitor MK-2206. Mice bearing xenograft tumors from orthotopic implantation of MCF7 cells were divided into four treatment groups: vehicle (DMSO), riluzole (10 mg/kg), MK-2206 (30 mg/kg) or a combination of riluzole (5 mg/kg), and MK-2206 (15 mg/kg) (single factor ANOVA, $n = 10$ for each treatment group, *error bars* represent SEM). **h** Proposed involvement of mGluR1 in breast cancer tumorigenesis. Glu, glutamate

Table 1

Percent of hollow lumen in dox-treated siGrm1-iMMEC and siGFP-iMMEC

Day 14	(−)Dox	(+)Dox
siGrm1	30 %	72 %
siGFP	30 %	18 %